Protein Cell 2010, 1(12): 1118–1127
DOI 10.1007/s13238-010-0144-5

Protein & Cell

RESEARCH ARTICLE

High affinity soluble ILT2 receptor: a potent inhibitor of CD8$^+$ T cell activation

Ruth K. Moysey[1,2*], Yi Li[1*], Samantha J. Paston[1], Emma E. Baston[1], Malkit S. Sami[1], Brian J. Cameron[1], Jessie Gavarret[1], Penio Todorov[1], Annelise Vuidepot[1], Steven M. Dunn[1,3], Nicholas J. Pumphrey[1,4], Katherine J. Adams[1], Fang Yuan[1], Rebecca E. Dennis[1], Deborah H. Sutton[1], Andy D. Johnson[1], Joanna E. Brewer[1,5], Rebecca Ashfield[1], Nikolai M. Lissin[1], Bent K. Jakobsen[1] ✉

[1] Immunocore Limited, 57c Milton Park, Abingdon, Oxon, OX14 4RX, UK
[2] Current address: Oxford Nanopore Technologies, UK
[3] Current address: Geneva Merck Serono S.A., Switzerland
[4] Current address: Adaptimmune Limited, UK
[5] Current address: Adaptimmune Limited, UK
✉ Correspondence: bent.jakobsen@immunocore.com
Received December 9, 2010 Accepted December 16, 2010

ABSTRACT

Using directed mutagenesis and phage display on a soluble fragment of the human immunoglobulin superfamily receptor ILT2 (synonyms: LIR1, MIR7, CD85j), we have selected a range of mutants with binding affinities enhanced by up to 168,000-fold towards the conserved region of major histocompatibility complex (MHC) class I molecules. Produced in a dimeric form, either by chemical cross-linking with bivalent polyethylene glycol (PEG) derivatives or as a genetic fusion with human IgG Fc-fragment, the mutants exhibited a further increase in ligand-binding strength due to the avidity effect, with resident half-times ($t_{1/2}$) on the surface of MHC I-positive cells of many hours. The novel compounds antagonized the interaction of CD8 co-receptor with MHC I *in vitro* without affecting the peptide-specific binding of T-cell receptors (TCRs). In both cytokine-release assays and cell-killing experiments the engineered receptors inhibited the activation of CD8$^+$ cytotoxic T lymphocytes (CTLs) in the presence of their target cells, with sub-nanomolar potency and in a dose-dependent manner. As a selective inhibitor of CD8$^+$ CTL responses, the engineered high affinity ILT2 receptor presents a new tool for studying the activation mechanism of different subsets of CTLs and could have potential for the development of novel autoimmunity therapies.

KEYWORDS CD8$^+$ T cells, cellular activation, autoimmunity, cell surface molecules, binding affinity, phage display

INTRODUCTION

The cytotoxic T lymphocyte (CTL) activation requires simultaneous binding of T-cell receptors (TCRs) and the CD8 co-receptor to the major histocompatibility complex (MHC) class I complex on the surface of a target cell. While the TCR engagement with the specific 8–11 amino acid residue-long antigenic peptides bound in the groove of MHC I (Willcox et al., 1999) is indispensable, growing evidence suggests that the importance of the CD8 contact during the course of CTL activation may vary, playing a more crucial role when antigens are presented at low copy number and/or toward which the TCR affinity is low (Gao and Jakobsen, 2000; Buslepp et al., 2003; Kerry et al., 2003; Bernardeau et al., 2005; Laugel et al., 2007; Zhang et al., 2010). This may open some new possibilities in the development of autoimmunity therapies, which, by disrupting the CD8 signaling route, would inhibit the activation of self-reactive low avidity CTLs, without significantly compromising the vital anti-viral

*These authors contributed equally to this work.

CTL responses. Soluble recombinant CD8αα has been shown to antagonize CTL activation (Sewell et al., 1999) and a very high sensitivity to the disruption of this pathway has been reported. However, because of the low affinity for MHC I (Wyer et al., 1999), high concentrations of soluble CD8αα were necessary.

Natural CD8 is predominantly a membrane-anchored heterodimer (CD8αβ) which makes contact with the relatively conserved α3 domain of the MHC I heavy chain, as well as the invariant β2m. Due to the difficulties involved in the engineering of higher affinity versions of CD8 (Cole et al., 2005), which both as αβ and αα forms binds MHC I in an asymmetrical fashion (Chang et al., 2006), we investigated the possibility of engineering an efficient CD8 binding antagonist based on a different framework. ILT2 (also known as LIR1, MIR7, CD85j) is a member of a family of inhibitory natural killer (NK) cell receptors known as the immunoglobulin-like transcript (ILT) family (Fanger et al., 1999), related to the killer-cell immunoglobulin-like receptor (KIR) family. ILT2 is expressed on a wide range of immune cells including MHC I-restricted $CD8^+$ T cells and subsets of NK cells (Borges and Cosman, 2000; Cella et al., 2000). It has been reported that ILT2 regulates human T cells by inhibiting CD3/TCR-mediated activation of both $CD4^+$ and $CD8^+$ T cell clones, and antigen recognition by $CD8^+$ cells (Saverino et al., 2000). The leukocyte inhibitory receptor family, to which ILT2 belongs, comprises eight closely related human proteins sharing 63% to 84% sequence identity with ILT2 (Fanger et al., 1999). Their extracellular regions contain either four or two immunoglobulin-like domains arranged linearly. Natural ILT2 consists of four extracellular domains and a cytoplasmic tail of four ITIMs, which mediate its cell-signaling effects (Hamerman and Lanier, 2006; Ivashkiv, 2009). Engagement of ILT2 triggers tyrosine phosphorylation of ITIMs and the subsequent recruitment of a number of protein tyrosine phosphatases (Binstadt et al., 1996), leading to downregulation of the signaling mediated by activating receptors (Colonna et al., 1997).

Unlike TCRs and KIRs, which interact with the polymorphic peptide-MHC surfaces, and similarly to CD8, ILT2 contacts the α3 and β2m domains of MHC I (Natarajan et al., 2002). It binds HLA-A, -B, -C and non-classical HLA-E, -F, -G with similar affinities and kinetics (Navarro et al., 1999; Lepin et al., 2000). Soluble ILT2, comprising the first two N-terminal domains (D1D2), exhibits a 20-fold higher affinity toward HLA A2, compared with that of CD8 (K_D ~7 μM *vs* K_D ~150 μM). Although the binding sites for CD8 and ILT2 on MHC I are mainly non-overlapping, steric exclusion prevents simultaneous binding of the two receptors to the same MHC I molecule (Willcox et al., 2003). Yet a much higher binding affinity would be required, if an ILT2-based compound were to serve as a therapeutic CD8 antagonist. We thus decided to investigate whether a high affinity version of ILT2 can be generated using protein engineering techniques, and whether such a molecule could efficiently downregulate CTL responses.

RESULTS

Engineering of high affinity ILT2 mutants

In this study we investigate the possibility of engineering a high affinity form of soluble ILT2 receptor to selectively inhibit the activation of $CD8^+$ T cells, as illustrated in the schematic model (Fig. 1A). Based on analyses of the unbound (Chapman et al., 2000) and the MHC I-bound (Willcox et al., 2002) crystal structures of the soluble two-domain ILT2 fragment, we have located several specific contact and non-contact areas in close proximity to the binding interface, which could contribute to the binding (Fig. 1B). We then created mutagenesis phage libraries, from which high affinity clones were identified using competition enzyme-linked immunosorbent assay (ELISA) with MHC I (HLA-A2) as the ligand. Following several rounds of positive selection, the mutants were subcloned into a T7 polymerase-based vector and expressed as inclusion bodies in *E. coli*. The variant proteins were made by refolding *in vitro* and purified to homogeneity by column chromatography, and their binding affinities toward MHC I were ranked using a surface plasmon resonance microchip-based detector, the Biacore 3000. From the first generation of libraries, affinity-enhancing mutations in different locations were combined to gain further increases in affinity. More than 40 individual variants were produced and analyzed on Biacore (data not shown). The properties of several key mutants, covering a broad range of binding affinities, are summarized in Table 1. With two lead candidates we examined whether the dramatic gains in affinity might have compromised the specificity of binding (Table 2). Despite the very large differences in the absolute values, the relative binding strengths of the tested variants, c64 and c138, toward a range of classical and non-classical human MHC I subtypes remained unchanged.

Design and properties of ILT2-based compounds

In addition to the ligand binding characteristics, the key factors influencing the design of a potential protein therapeutic include its ease of production, stability, and pharmacokinetic (PK) profile. We found that all the picomolar affinity mutants, exemplified by c132 (Table 1), exhibited higher levels of non-specific aggregation and were generally less stable (data not shown). Based on their biochemical properties, several mutants, c50, c57, c64, c132 and c138, were investigated further. The relatively small molecular mass (MM, 22 kDa) of the soluble two-domain ILT2 fragment, which is significantly below the kidney filtration threshold, dictates the necessity of PK-enhancing modifications. We decided on the dimeric protein format, bearing in mind the potential

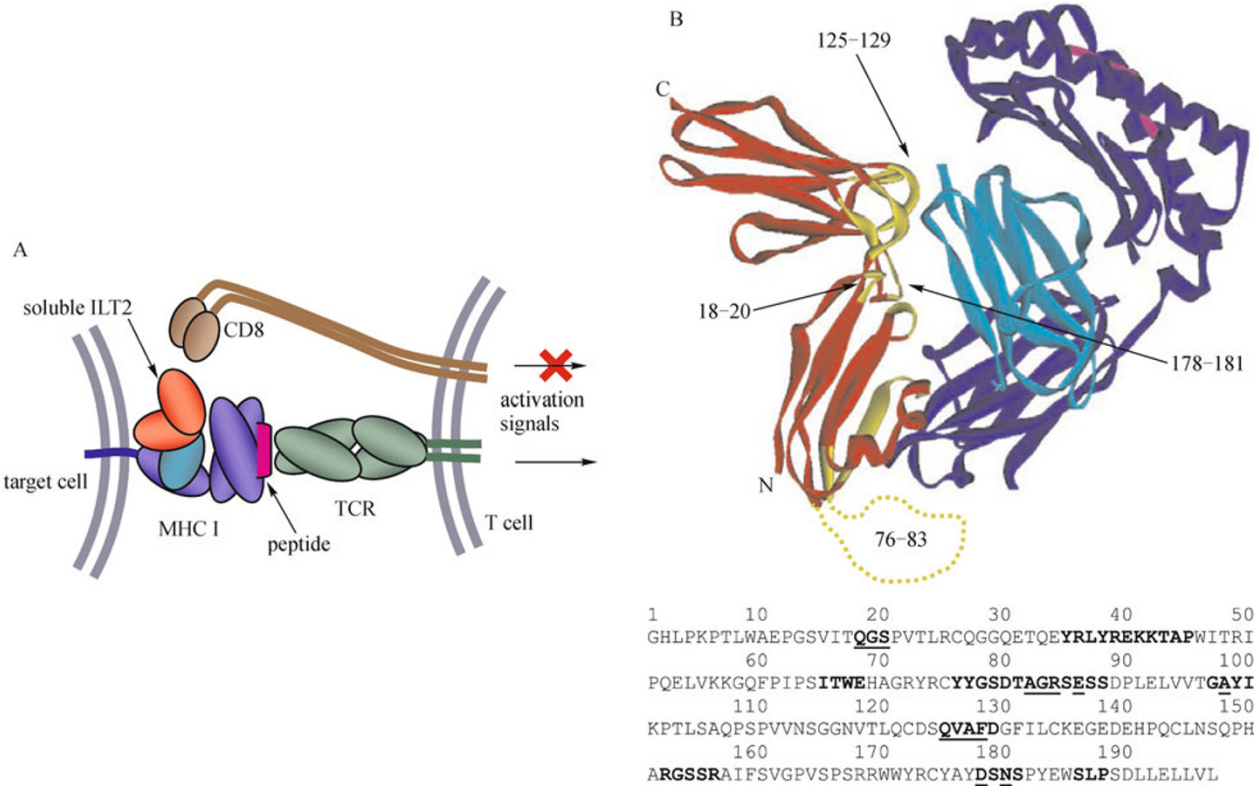

Figure 1. Engineering of ILT2-based antagonist of CD8 co-receptor. (A) Concept sketch. Soluble ILT2 binds to conserved region of major histocompatibility complex I (MHC I), blocking its contact with CD8. Binding of T cell receptor (TCR) alone to the antigenic peptide presented on MHC I is insufficient for cytotoxic T lymphocyte (CTL) activation. (B) Crystal structure-based model of soluble ILT2 (immunoglobulin-like transcript 2) bound to peptide-MHC I complex. The MHC heavy chain is shown in blue, β2m in cyan, and antigenic peptide in pink. ILT2 domains, D1 (N-terminal) and D2, are shown in red, and N- and C- termini are indicated. Parts of the ILT2 chain, which have been subjected to mutagenesis, are shown in yellow. Numbers indicate the areas wherein mutation contributed to increased affinity. (Part of the ILT2 structure unresolved by X-ray crystallography is shown as a dotted loop.) On the corresponding wild type amino acid pane (bottom) the mutated areas are highlighted and the positions of affinity-enhancing mutations underlined. For bacterial expression a methionine-encoding start codon was added and the C-terminal sequence LVL was changed to DVDG to improve folding and stability of the protein.

benefits for the PK characteristics (owing to the increased size), as well as the possibility of a further gain in ligand binding strength due to the avidity effect (Fig. 2A). First, we made soluble high affinity ILT2 dimers by chemical cross-linking with bi-valent polyethylene glycol (PEG) derivatives. ILT2 polypeptides were engineered with an unpaired C-terminal cysteine residue, with which bis-maleimide substituted PEGs react highly selectively, resulting in a defined dimeric product. Second, we engineered a fusion of select high affinity ILT2 variants with the naturally dimerizing human IgG-derived Fc fragment. The dimers were Biacore tested and exhibited dramatically enhanced binding to MHC I compared with their corresponding monomers (Fig. 2B). We then tested whether the binding of high affinity ILT2 dimers to MHC I prevented the subsequent binding of CD8 (Fig. 2C). The high affinity ILT2 completely blocked the binding of soluble CD8, but did not prevent the binding of soluble TCRs specific for the peptide-MHC I complex. We further investigated, using a soluble TCR/peptide-MHC I pair, whether a quantitative effect (e.g. a change in affinity) on TCR binding may result from the high affinity ILT2 dimers engagement with MHC I. No statistically significant effect on TCR binding was observed and thus high affinity ILT2 binding to MHC I does not affect the contact with TCRs (Fig. 2D).

Fluorescence microscopy and flow cytometry were used to demonstrate the ability of ILT2-derived compounds to bind MHC I complexes on the cell surface. Human peripheral blood mononuclear cells (PBMCs) and the MHC I-negative cell line K562 were incubated with c138-Fc dimers, followed by a protein A-FITC conjugate treatment. Easily detectable staining was observed on PBMCs, while the K562 cells remained unstained (Fig. 2E). The residence time of c138-Fc

Table 1 Selected ILT2 variants and their HLA-A2 binding properties

	18–20	76–83	97–100	125–129	178–181	K_D	$t_{1/2}$
WT	QGS	YYGSDTAGRSESS	GAYI	QVAFD	DSNS	6.9 μM	ND
c50	**MDQ**	YYGSDT**SQW**S**A**SS	G**V**YI	QVAFD	DSNS	45 nM	7 s
c57	**LQS**	YYGSDT**SQW**S**A**SS	G**V**YI	QVAFD	DSNS	42 nM	15 s
c64	**MDQ**	YYGSDT**RQW**S**A**SS	G**V**YI	QVAFD	DSNS	40 nM	15 s
c138	**MDQ**	YYGSDT**RQW**S**A**SS	G**V**YI	**PFQA**D	DSNS	2.6 nM	2.4 min
c132	**MDQ**	YYGSDT**SQW**S**A**SS	G**V**YI	**PFQA**D	**M**S**W**S	41 pM	132 min

Substitutions within the amino acid sequence are shown in bold for each construct. ILT2, immunoglobulin-like transcript 2; HLA, human leukocyte antigen.

Table 2 Binding properties of two ILT2 variants toward a range of classical and non-classical MHC I complexes

MHC I subtype	K_D c64 (nM)	$t_{1/2}$ c64 (s)	$t_{1/2}$ c138 (s)
HLA-A1	22	19	263
HLA-H2	41	15	167
HLA-A3	66	20	194
HLA-A24	17	21	292
HLA-B8	18	21	299
HLA-B27	17	21	ND
HLA-Cw6	21	24	630
HLA-G	15	18	289
HLA-E	11	12	237

ILT2, immunoglobulin-like transcript 2; MHC, major histocompatibility complex; HLA, human leukocyte antigen.

dimers on human PBMCs, determined in a time-course experiment, revealed a relatively stable interaction with a half-life exceeding 24 h (Fig. 2F).

Inhibition of peptide-specific CTL responses

To test the ability of the engineered ILT2 compounds to inhibit CTL responses we used a T cell clone specific for the cancer-related MelanA peptide ELAGIGILTV, with the Mel 624 melanoma tumor cell line as targets. In our initial experiments we have investigated whether oligomerization could increase the potency of the ILT2 compounds. In an INFγ release assay, inhibition by a PEGylated dimer was about 50-fold stronger, and by a PEGylated tetramer some 200-fold stronger, compared with the inhibition by the corresponding monomers (Fig. 3A). Considering the difficulties in producing uniform PEGylated tetramers, we decided to concentrate on the dimeric protein format. The inhibition of IFNγ release from the T cell clone by dimeric ILT2 compounds (Fig. 3B) showed dose dependence, with complete inhibition achievable at concentrations in the range of 10 nM–1 μM. Cellular IC_{50} (half maximal inhibitory concentration) values were obtained by titrating the amount of added inhibitor, and were found to correlate with the measured affinities of the corresponding monomers, with the higher affinity compounds performing generally better than the lower affinity ones. However, little or no difference in the potency was observed between the two top-ranking mutants, c132 and c138, despite their affinities differing more than 50-fold. No difference in potency was observed when PEG- and Fc-based dimers of the same ILT2 variant were tested against each other. We further studied the ability of c138-Fc to inhibit the release of other inflammatory cytokines, such as IL-2, tumor necrosis factor-alpha (TNFα) and macrophage inflammatory protein-1β (MIP-1β) from the CTL clone (Fig. 3C). As with IFNγ (used here as a reference), dose dependent curves were obtained in all cases, with sub-nanomolar (IL-2, MIP-1β) or low nanomolar (TNFα) cellular IC_{50} values. The inhibition of killing of Mel 624 cells by the CTL clone in the presence of c64-, c132- and c138-based compounds was also investigated (Fig. 3D). In agreement with the IFNγ release data, the cell-killing inhibition showed dose dependence, with the higher affinity ILT2 variants being more potent inhibitors. However, the two highest affinity mutants (c132 or c138) required the same concentration (about 100 nM) for complete inhibition of the cell killing.

DISCUSSION

Phage display technology is used routinely to increase the binding affinity of monoclonal antibodies for their corresponding antigens (McCafferty et al., 1990; Clackson et al., 1991; Chang et al., 2006). More recently, it has been adapted to select high affinity variants of soluble TCRs (Li et al., 2005; Dunn et al., 2006). Our results here show how this technique can be applied to a new type of immunological receptor. Contrary to immunoglobulin and TCR molecules, where the affinity enhancing mutagenesis is directed toward a limited number of well defined hypervariable loops (CDRs), choosing the mutagenesis targets on ILT2 presented a considerable challenge. The 7 contact loops which can be seen on the crystal structure of HLA A2-bound ILT2 (Willcox et al., 2003) (Fig. 1B) could indisputably be important for the binding. However, through molecular modeling we have identified two more regions with a potential for the affinity maturation. Subsequently, all these areas have been mutated, of which 5

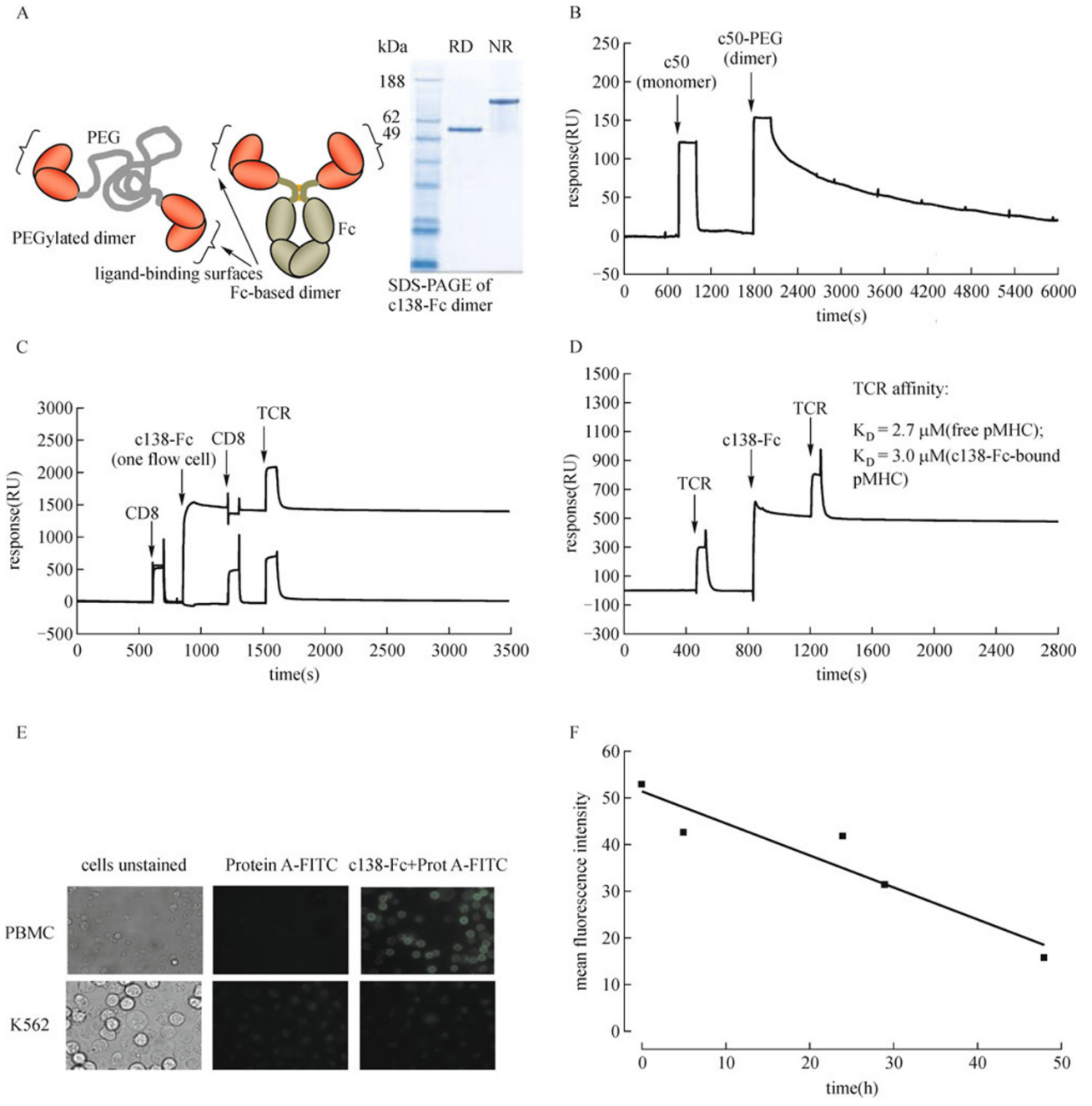

Figure 2. Design and the ligand binding properties of soluble ILT2 dimers. (A) Dimeric ILT2-based compounds: schematic representation of chemically cross-linked with PEG (left) *vs* genetically fused with the immunoglobulin Fc-domain (center). A sodium dodecyl sulfate polyacrylamide gel electrophoresis (SDS-PAGE) of a c138-Fc dimer sample under reducing and non-reducing conditions is also shown (right). (B) The binding of dimeric *vs* monomeric ILT2 c50 to MHC I (HLA-A2). Dimerization resulted in a dramatic enhancement of the ligand binding strength, with the $t_{1/2}$ increase from 7 s in c50 monomer to about 80 min in c50-PEG dimer. RU, response unit. (C) High affinity dimeric ILT2 prevents the interaction of CD8 with MHC I. CD8 binds with low affinity to MHC I. Injected over one flow cell, high affinity dimeric ILT2 (c138-Fc) binds to MHC I very strongly, cancelling the subsequent binding of CD8, but with no effect on the binding of the peptide-specific TCR. (D) High affinity dimeric ILT2 (c138-Fc) does not affect the binding affinity of TCR toward peptide-MHC I. Biacore trace illustrates the binding of a TCR (HTLV-1 Tax-specific) to its relevant peptide-MHC I, before and after the binding of c138-Fc. K_D values, derived from equilibrium binding (not shown on the trace), were 2.7 μM (free peptide-MHC I as ligand) *vs* 3.0 μM (c138-Fc bound ligand), which is not statistically different. (E) Visualization, using fluorescence microscopy, of the high affinity dimeric ILT2 (c138-Fc) on the surface of MHC I expressing cells. MHC I-negative cell line, K562, served as control. (F) Time course of dissociation from cells of high affinity dimeric ILT2 (c138-Fc) measured by flow cytometry ($t_{1/2}$ > 24 h). ILT2, immunoglobulin-like transcript 2; MHC, MHC, major histocompatibility complex; HLA, human leukocyte antigen; TCR, T cell receptor.

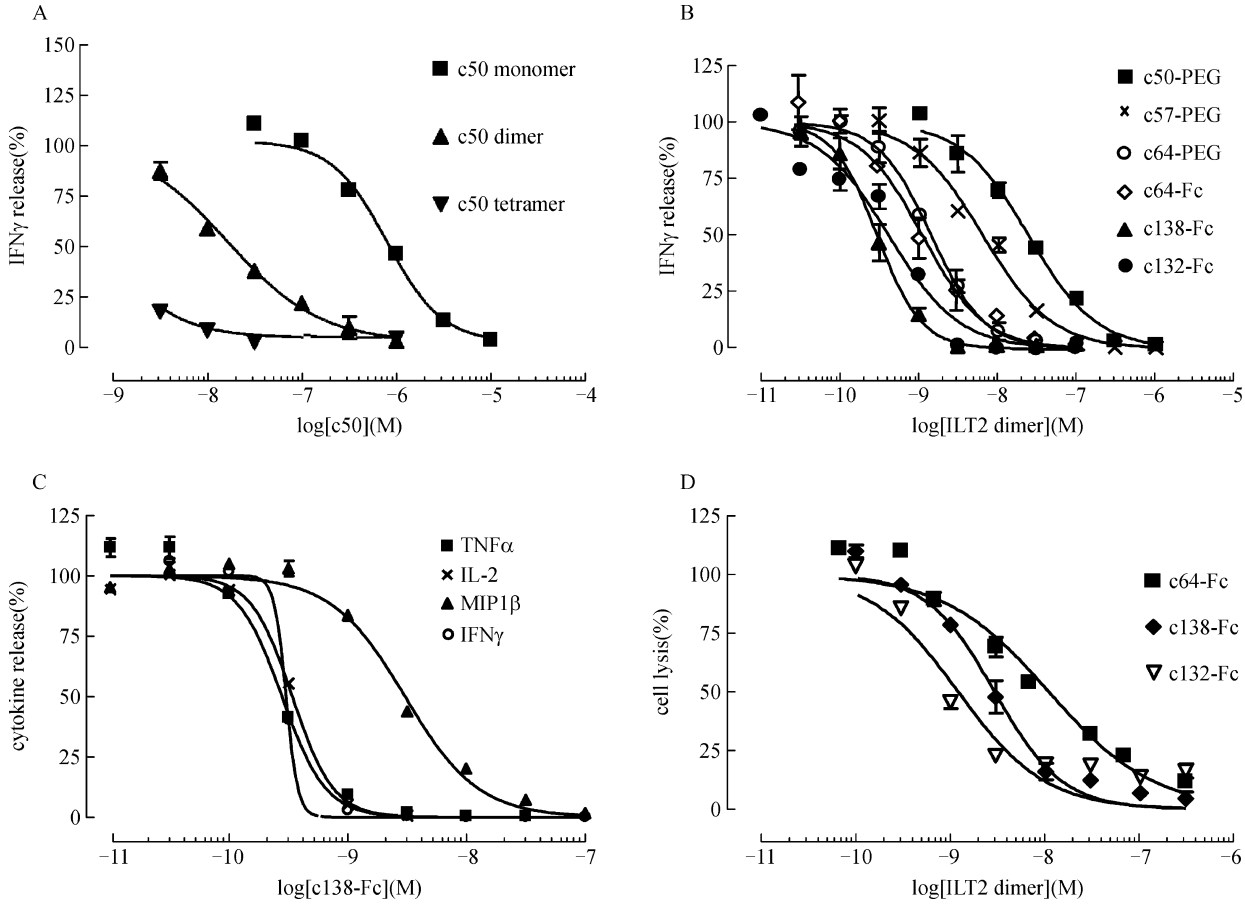

Figure 3. Inhibition of CTL responses by high affinity ILT2. (A) Inhibition by ILT2 compounds of interferon γ (IFNγ) release from a CTL clone in the presence of target cells: monomeric *vs* dimeric *vs* tetrameric ILT2 c50. (B) Inhibition by ILT2 dimers of IFNγ release by a CTL clone in the presence of the target cells: affinity effect on potency. (C) Inhibition by c138-Fc of the release of inflammatory cytokines IL-2, tumor necrosis factor alpha (TNFα), IFNγ and MIP-1β. (D) Inhibition by ILT2 compounds of the killing of target cells by a CTL clone. MIP-1β, macrophage inflammatory protein-1β. The other abbreviations are the same as in Fig. 1 and 2.

areas generated mutants exhibiting significant increases in binding affinity. Three of these loci (aa 18–20, aa 97–100, and aa 125–129) represented loops extending toward the invariant β2m. The fourth one (aa 178–181) was a non-contact loop facing a large water-filled cavity on the interface between β2m and the α3 domain of HLA I. Mutations in this area, notably the inclusion of large hydrophobic residues, could contribute to stronger binding by displacing water molecules from the cavity. Finally, the fifth locus was identified in an area that is unresolved in the crystal structures (aa 76–81), suggesting it has a high degree of flexibility. While the precise configuration of this loop is unknown, its proximity to the α3 domain of HLA I explains the importance of this region. Individual mutations in the above regions contributed to the enhancement in the binding affinity in the range of 10–60 folds (data not shown). As observed with the mutagenesis on the CDRs of monoclonal antibodies and TCRs, combining mutations in more than one loop generally had an additive and synergistic effect, achieving a maximal improvement in the ligand binding affinity of almost 170,000-fold (K_D = 41 pM for c132 *vs* K_D = 6.9 μM for the wild type receptor). Importantly, the profound gains in binding affinity did not alter the specificity of the interaction, as was determined for a representative set of classical and non-classical MHC Is (Table 2), between which the affinity values varied no greater than 4.4-fold. Considering the relatively high conservation of the α3 domains between the HLA I subtypes, and especially the fact that 3 out of 5 mutated ILT2 loops contacted the invariant β2m, the latter was not unexpected. No binding toward MHC II was detected in any of tested ILT2 mutants (data not shown).

Both PEGylation and genetic fusions are commonly used as PK-enhancing modifications of biopharmaceuticals (Veronese and Mero, 2008). Attachment to a protein molecule of

one or several hydrophilic and biologically inert polyethylene glycol chains is known to prolong residence times in the body, improve resistance against proteolysis, and reduce immunogenicity and non-specific toxicity. PEGs of various sizes (2–40 kDa), configurations (linear *vs* branched), attachment chemistries and valences (mono-, bi-, tetra-) are commercially available (Gaberc-Porekar et al., 2008). The choice of bis-maleimide substituted PEGs (Roberts et al., 2002) provided the advantage of producing uniform, chemically defined ILT2 dimers, with only a minor contamination by PEGylated ILT2 monomer. Due to the non-structured nature of PEG, the gain in the protein molecule's apparent size (diffusion radius) exceeds that calculated directly from the increase in molecular mass (Fee and Van Alstine, 2004). The effect could easily be observed during size-exclusion chromatography where the ILT2 dimer made with 3.4 kDa PEG (combined MW 48.4 kDa) behaved similarly to a much larger protein of approximately 80 kDa (data not shown). As expected, the dimers exhibited a greatly enhanced ligand binding strength compared with the monomers. The simplicity of the PEGylation technique has allowed us to quickly produce all of our key mutants in the dimeric form for cellular experiments. In comparison, producing the protein as a genetic fusion with a self-dimerizing immunoglobulin Fc fragment offered the advantage of consistency, through production of large batches from mammalian cell expression. Three lead candidates, c64, c132 and c138 have been produced as Fc-dimers. Measured on Biacore, the ligand binding characteristics of these molecules were indistinguishable from those of their PEGylated counterparts (data not shown). This observation was somewhat surprising, bearing in mind the significantly more rigid structure of an Fc-fusion, as opposed to the randomly fluctuating configuration of the PEGylated dimer. It is clear that bivalent binding occurred predominantly in both cases suggesting that the immobilized ligand density was not limiting for the more tightly spaced 'arms' of Fc-dimers.

To function as a CD8 co-receptor antagonist *in vivo*, high affinity ILT2 must be able to exclude CD8 binding through steric hindrance, bearing in mind that the binding surfaces for the two receptors on MHC I are mostly non-overlapping. We have provided experimental evidence in support of this model, as the binding of CD8αα homodimer to HLA-A2 was completely abrogated in the presence of the ILT2 dimers (Fig. 2C). While physiologically CD8αα is non-identical to the natural CD8αβ heterodimer (McNicol et al., 2007), its binding to MHC I mimics one of the two proposed modes of the CD8αβ binding (Chang et al., 2006) and is capable of antagonizing the latter (Sewell et al., 1999). The peptide-specific binding of TCR is unaffected by the bound CD8αα (Wyer et al., 1999). Similarly, the binding of high affinity ILT2 compounds did not interfere with the TCR binding (Fig. 2C). To examine this notion quantitatively, we measured the TCR equilibrium binding affinities before and after the addition of high affinity ILT2 and found no statistically significant difference in the two K_D values. The binding of high affinity ILT2 thus antagonized the binding of CD8αα to MHC I complexes, leaving the peptide-specific binding of TCR to the same complex unaffected.

The selection of a number of ILT2 variants, spanning a broad affinity range, provided us with an opportunity to study the affinity-driven physiologic effects of the engineered molecules using CTL activation as a model. Our initial experiments have shown that the PEGylated c50 dimer was about 50-fold more potent than the corresponding monomer, while the PEGylated c50 tetramer was at least 4-fold more potent than the dimer. Additionally, PEGylated c64 dimer was significantly more potent compared with monomeric c138, despite the fact that the latter has a much higher affinity than monomeric c64 (data not shown). This implies that avidity-enhanced, i.e. multi-valent, interactions of the ILT2 compounds with MHC I complexes on the surface of the target cells play an important role in the inhibition. In agreement with the binding data, no noticeable difference in potency was observed between the PEGylated dimers and their Fc-based counterparts. In all cases, a dose-dependent inhibition of target cell-driven activation of $CD8^+$ CTLs was observed. As expected, higher affinity mutants were progressively more potent inhibitors compared with their lower affinity counterparts, as measured in the cytokine release and cell-killing assays (Fig. 3B and 3D). In certain cases, however, the above generalization does not apply. Notably, c64-based dimer showed a stronger inhibition than its c57-based counterpart, despite their near identical ligand binding properties. One possible explanation would be dissimilar stabilities of the two compounds under the conditions of the experiment. No statistically relevant difference in the cytokine release inhibition was observed between the two highest affinity mutants, c138 and c132, despite a significant difference in their affinities. Furthermore, while the c132-based dimer appeared to be overly the most potent inhibitor in the cell killing assay, no salient difference between c132-Fc and c138-Fc was observed in the range of concentrations causing complete inhibition. This suggests a saturating (plateau) effect, where no further increase in the binding strength translates into increased potency, perhaps when too few ligands are left unoccupied for CTL activation to occur. It is important to note, though, that raising the activation threshold, as opposed to the complete inhibition, must be crucial in achieving a balanced physiologic effect *in vivo*.

The range of ILT2 derived compounds with different affinities toward HLA I described in this work presents a unique tool for studying the activation of CTLs and its dependence upon the CD8 signaling. Moreover, and potentially of much higher importance, our results demonstrate the possibility, in principle, of engineering of a highly potent CD8 antagonist for therapeutic purposes.

MATERIALS AND METHODS

Library construction and screening

A gene fragment encoding the wild-type ILT2 polypeptide, comprising the amino acid residues 1–196, was made by Geneart. The gene was subcloned into a phagemid vector pEX922 (Li et al., 2005; Dunn et al., 2006), so that the protein product became fused, via its C terminus, with the gene III of the bacteriophage M13. The mutagenesis regions were identified through molecular modeling. Library DNA was generated by using PCR amplification with mutagenic oligonucleotides as forward primers and downstream complementary oligonucleotides as reverse primers, stitching the overlapping fragments to form the complete gene, and ligating into the pEX922 vector. Electroporation into *E. coli* TG1 cells and subsequent library phage rescue was carried out according to the standard protocols. All libraries were of sufficient size, typically 10^8, to cover theoretically encoded repertoires. The phage display was performed essentially according to the previously published methods (Li et al., 2005; Dunn et al., 2006), with the phage packaging carried out at 37°C. Biotinylated and non-biotinylated soluble peptide-MHC complexes were prepared as previously described (Garboczi et al., 1992). We performed panning of the phage libraries against human peptide-MHC-A2 (pHLA-A2) complexes captured on MaxiSorp Immunotubes (Nunc) and streptavidin-coated magnetic beads as described previously (Li et al., 2005). To bias the selection in favor of higher affinity mutants, the panning for 2nd or 3rd generation libraries was carried out using solution equilibrium binding. Rescued phages were blocked using 3% Marvel dried milk in PBS and then incubated in solution with 10–100 nM biotinylated pHLA-A2 complex. After 1 h, pre-blocked streptavidin-coated magnetic beads were added and complexes captured by magnetic precipitation. Eluted phage was used to infect mid-log phase TG1 cultures and infected cells were precipitated and grown on agar plates containing ampicillin and glucose. Subsequently ILT2-displaying phage particles were rescued from the cells and were fed back into the next cycle of selection. In total, 3–4 cycles of selection were performed for each library. Individual clones were screened initially by ELISA, and confirmed positives were further assayed by soluble inhibition ELISA using various concentrations of pHLA-A2 complex.

Recombinant protein production

Isolated mutants were cloned into the expression vector pGMT7. The expression and the inclusion bodies purification was done essentially as described previously (Willcox et al., 1999). Inclusion bodies (30 mg protein) were denatured in 20 mL guanidine buffer (6 M guanidine-HCl, 50 mM Tris-HCl, pH 8, 100 mM NaCl, 10 mM EDTA, 20 mM DTT) for approximately 30 min at 42°C before addition to 1 L of cold, rapidly stirred refolding buffer (100 mM Tris-HCl, pH 8, 400 mM L-arginine, 2 mM EDTA, 15% glycerol, 0.7 g/L cystamine and 3 g/L 2-cysteamine), followed by a dialysis against 20 L of 10 mM Tris, pH 8, over two days with two changes of the buffer. Dialysed protein was filtered to remove precipitated material, loaded onto a Q-Sepharose anion-exchange column (GE Healthcare) and eluted with a NaCl gradient in 25 mM Tris-HCl, pH 8. Peak fractions were pooled and concentrated using Vivaspin concentrators (Sartorius). The protein was further purified by size-exclusion chromatography on a Superdex S75 column (Pharmacia) in PBS. Peak fractions were analyzed by SDS-PAGE. Protein concentration was measured from UV spectra, using an absorbance coefficient (A_{280}) calculated individually for each mutant.

Surface plasmon resonance

The binding of ILT2 to pHLA complexes was studied using a surface plasmon resonance microchip-based detector, Biacore3000 (Biacore). Biotinylated pHLA was captured via covalently coupled streptavidin onto the CM5 chip. To measure K_D in equilibrium experiments, a range of 2-fold dilutions of the tested protein were injected over the immobilized pHLA at a flow rate of 5 μL/min and the ligand density of approximately 500 response units (RU). Kinetic experiments were carried out with a low ligand density (~200 RU) and a high flow rate of 50 μL/min. Equilibrium data were fitted with a hyperbolic model using Biaevaluation software (Biacore). Association and dissociation rate constants (where applicable) were calculated from the kinetic data, as well as the dissociation half time values ($t_{1/2}$). Soluble TCR and CD8 proteins used in some experiments were made as described previously (Sewell et al., 1999; Willcox et al., 1999).

Production of ILT2 dimers

To make PEGylated dimers, selected ILT2 mutants were engineered with an extra C-terminal cysteine. The protein was mildly reduced by incubating overnight at 4°C in the presence of 0.05 mM TCEP (Pierce). A bis-maleimide PEG, SUNBRIGHT DE-034MA (NOF Corporation) dissolved in dimethyl formamide was added in several aliquots with 10 min intervals, allowing the maleimide residues to react with free thiols. The total added amount of PEG was calculated so that the maleimide to thiol ratio was slightly below equimolar. The products were separated on a Superdex S200 column (Pharmacia) and analyzed by SDS-PAGE. The dimer fraction was free from non-reacted monomer and typically showed a slight contamination with PEGylated monomer. Pegylated ILT2 tetramers (used in the initial experiments) were made analogously, using a tetra maleimide-substituted PEG derivative. Fc-fusion constructs were engineered for three ILT2 lead candidates, c64, c138 and c132, covering a wide affinity range. A human IgG1-derived Fc, mutated to abrogate antibody-dependent cell-mediated cytotoxicity (ADCC) and complement-dependent cytotoxicity (CDC) was used to impart on the Fc-fusion protein desirable safety and high yield manufacture characteristics. Batches of each fusion construct have been manufactured at a GMP (good manufacturing practice) compliant facility using standard CHO cell expression systems and Protein A purification methodologies.

Cell lines

Mel 624 melanoma cell line was obtained from Thymed, and K562 cells were purchased from DSMZ Human and Animal Cell Lines Database. Cells were maintained in R10 medium (RPMI-1640 medium with 2 mM L-glutamine, 100 μg/mL penicillin and 100 μg/mL streptomycin, supplemented with 10% FCS). To generate a Melan A-specific T cell clone, PBMCs from a healthy HLA-$A2^+$ donor were isolated and stimulated in the presence of IL-7 by autologous antigenic presentation, using the Melan $A_{26–35}$ ELAGIGILTV heteroclitic peptide at 10 μM. Three days after the initial antigen exposure, IL-2 was gradually added to the culture up to 100 U/mL. Rounds of restimulation were repeated every 12–14 d. Following successful

expansion, antigen-specific cells were sorted by flow cytometry using a BD FACSVantage machine (BD Biosciences) on the basis of the tetramer and CD8 positivity. Double positive cells were sorted and grown for 2–3 weeks in R10 medium containing 10% T-STIM (BD Biosciences) and 100 U/mL IL-2, in the presence of mixed irradiated allogeneic feeders from three unrelated donors. The antigenic specificity of the clone was then tested by the tetramer staining, an IFNγ ELISPOT assay and a cell-killing assay.

Cell staining with ILT2-Fc

An imaging system (Universal Imaging Corporation), based upon a Zeiss Axiovert 200 M automated inverted microscope, equipped with a 63 × objective lens and a filter set (Zeiss), consisting of BP450–490 (excitation), FT510 (beam splitter) and LP515/565 (emission) filters, was used for detecting FITC fluorescence. For staining with high affinity ILT2, 1 × 10^6 cells were aliquoted per tube, washed and resuspended in 100 µL staining buffer (PBS + 2% fetal calf serum, Gibco), after which 5 µg ILT2 was added per tube, followed by the incubation for 30 min in the dark at 4°C. The cells were washed twice and resuspended in a 100 µL staining buffer, FITC-Protein A (Zymed Laboratories) added to each tube at 10 µg/mL in staining buffer, followed by the incubation in the dark at 4°C. Finally, the cells were washed twice in staining buffer and resupended in 100 µL minimal imaging medium (R-10 lacking phenol red) and 10 µL of this was then transferred to eight-well chambered coverslips (Nunc), ready for imaging. To measure the cellular off rate, the cells were stained with ILT2 as described above, resuspended in R10 medium and incubated in 24 well plates at 37°C and 5% CO_2 for the time period stated, stained with Protein A-FITC as above and placed on ice before analysis by flow cytometry, which was carried out using an FC500 Beckman Coulter machine.

Cytokine release assays

For the IFNγ ELISPOT assays (Diaclone), PVDF membrane plates were coated with anti-human IFNγ capture antibody and blocked according to the manufacturer's instructions. Target cells were plated out in 50 µL R10 medium into the pre-coated plates at 50,000 cells/well. Tested ILT2 compound was added to the wells at varying concentrations in 50 µL R10 medium and the plates were incubated at room temperature for 20 min. Effector cells were added at 500–1000 cells/well in 50 µL R10 and the plates incubated overnight at 37°C/5% CO_2. Effector cells alone, target cells alone and effectors plus targets were run as assay controls. The plates were developed according to manufacturer's instructions and evaluated on a CTL Immunospot Series 4 ELISPOT Analyzer. For TNFα, IL-2, IFNγ Eli-pair assays (Diaclone, IDS Ltd) and MIP-1β DuoSet ELISA assays (R&D Systems), experiments were set up in 96 well round bottom plates (Nunc), following the same protocol as the ELISPOT assays, but plating 50,000 target cells/well and 5000 effector cells/well. After incubating overnight at 37°C/5%CO_2, the plates were spun at 300 g to pellet cells, and the supernatants assayed for the cytokine concentrations in ELISAs according to the manufacturer's protocols. Data were analyzed using Prism 4.0 software (GraphPad Software).

Cell-killing assay

Cell killing was evaluated using non-radioactive DELFIA assay (PerkinElmer) according to the manufacturer's protocols. 1–3 µL BATDA reagent was added to 1×10^6 target cells in 1 mL assay medium (R10) followed by incubation for 30 min at 37°C/5%CO_2. The cells were washed three times and resuspended in the assay medium with 100 µM β-ME at 1×10^5 cells/mL, to give 5,000 cells/well in 50 µL in a 96-well round-bottom plate (Nunc). Tested ILT2 compounds were added to the wells at varying concentrations in 50 µL assay medium, before the addition of effector cells at 15,000 cell/mL in 50 µL assay medium, giving an effector to target ratio of 3:1. Target cells alone (spontaneous release), target cells with 1% Triton × 100 (maximum release) and the supernatant from the final wash of the targets (background) were used as assay controls. The plates were incubated at 37°C/5%CO_2 for 2 h, then centrifuged, and 20 µL of supernatant transferred to a 96 well flat-bottom black plate (Nunc). 180 µL Europium solution was added to each well and the plates shaken for 15 min, before reading in a Wallac Victor-2 multilabel plate reader (PerkinElmer). The spontaneous release (%) = 100 × (spotaneous release– background)/(maximum release – background); the assay was only accepted if the spontaneous release was less than 30%. Specific lysis (%) = 100 × (experimental release – spontaneous release)/(maximum release – spontaneous release).

ACKNOWLEDGEMENTS

This work was funded by MediGene AG, Munich, Germany. Authors declare no conflict of interest associated with this work.

ABBREVIATIONS

ADCC, antibody-dependent cell-mediated cytotoxicity; BCIP, 5-bromo-4-chloro-3′-indolyphosphate p-toluidine; CDC, complement-dependent cytotoxicity; CTL, cytotoxic T lymphocyte; ELISA, enzyme-linked immunosorbent assay; IC_{50}, half maximal inhibitory concentration; ILT, immunoglobulin-like transcript; IPTG, isopropyl β-D-1-thiogalactopyranoside; MHC, major histocompatibility complex; MIP-1β, macrophage inflammatory protein-1β; PEG, polyethylene glycol; PK, pharmacokinetic; PVDF, polyvinylidene fluoride; TCEP, tris(2-carboxyethyl)phosphine; TCR, T-cell receptor

REFERENCES

Bernardeau, K., Gouard, S., David, G., Ruellan, A.L., Devys, A., Barbet, J., Bonneville, M., Cherel, M., and Davodeau, F. (2005). Assessment of CD8 involvement in T cell clone avidity by direct measurement of HLA-A2/Mage3 complex density using a high-affinity TCR like monoclonal antibody. Eur J Immunol 35, 2864–2875.

Binstadt, B.A., Brumbaugh, K.M., Dick, C.J., Scharenberg, A.M., Williams, B.L., Colonna, M., Lanier, L.L., Kinet, J.P., Abraham, R.T., and Leibson, P.J. (1996). Sequential involvement of Lck and SHP-1 with MHC-recognizing receptors on NK cells inhibits FcR-initiated tyrosine kinase activation. Immunity 5, 629–638.

Borges, L., and Cosman, D. (2000). LIRs/ILTs/MIRs, inhibitory and stimulatory Ig-superfamily receptors expressed in myeloid and lymphoid cells. Cytokine Growth Factor Rev 11, 209–217.

Buslepp, J., Kerry, S.E., Loftus, D., Frelinger, J.A., Appella, E., and Collins, E.J. (2003). High affinity xenoreactive TCR:MHC interaction recruits CD8 in absence of binding to MHC. J Immunol 170, 373–383.

Cella, M., Nakajima, H., Facchetti, F., Hoffmann, T., and Colonna, M. (2000). ILT receptors at the interface between lymphoid and myeloid cells. Curr Top Microbiol Immunol 251, 161–166.

Chang, H.C., Tan, K., and Hsu, Y.M. (2006). CD8alphabeta has two distinct binding modes of interaction with peptide-major histocompatibility complex class I. J Biol Chem 281, 28090–28096.

Chapman, T.L., Heikema, A.P., West, A.P. Jr, and Bjorkman, P.J. (2000). Crystal structure and ligand binding properties of the D1D2 region of the inhibitory receptor LIR-1 (ILT2). Immunity 13, 727–736.

Clackson, T., Hoogenboom, H.R., Griffiths, A.D., and Winter, G. (1991). Making antibody fragments using phage display libraries. Nature 352, 624–628.

Cole, D.K., Rizkallah, P.J., Sami, M., Lissin, N.M., Gao, F., Bell, J.I., Boulter, J.M., Glick, M., Vuidepot, A.L., Jakobsen, B.K., *et al.* (2005). Crystallization and preliminary X-ray structural studies of a high-affinity CD8alphaalpha co-receptor to pMHC. Acta Crystallogr Sect F Struct Biol Cryst Commun 61, 285–287.

Colonna, M., Navarro, F., Bellon, T., Llano, M., Garcia, P., Samaridis, J., Angman, L., Cella, M., and Lopez-Botet, M. (1997). A common inhibitory receptor for major histocompatibility complex class I molecules on human lymphoid and myelomonocytic cells. J Exp Med 186, 1809–1818.

Dunn, S.M., Rizkallah, P.J., Baston, E., Mahon, T., Cameron, B., Moysey, R., Gao, F., Sami, M., Boulter, J., Li, Y., *et al.* (2006). Directed evolution of human T cell receptor CDR2 residues by phage display dramatically enhances affinity for cognate peptide-MHC without increasing apparent cross-reactivity. Protein Sci 15, 710–721.

Fanger, N.A., Borges, L., and Cosman, D. (1999). The leukocyte immunoglobulin-like receptors (LIRs): a new family of immune regulators. J Leukoc Biol 66, 231–236.

Fee, C.J., and Van Alstine, J.M. (2004). Prediction of the viscosity radius and the size exclusion chromatography behavior of PEGylated proteins. Bioconjug Chem 15, 1304–1313.

Gaberc-Porekar, V., Zore, I., Podobnik, B., and Menart, V. (2008). Obstacles and pitfalls in the PEGylation of therapeutic proteins. Curr Opin Drug Discov Devel 11, 242–250.

Gao, G.F., and Jakobsen, B.K. (2000). Molecular interactions of coreceptor CD8 and MHC class I: the molecular basis for functional coordination with the T-cell receptor. Immunol Today 21, 630–636.

Garboczi, D.N., Hung, D.T., and Wiley, D.C. (1992). HLA-A2-peptide complexes: refolding and crystallization of molecules expressed in Escherichia coli and complexed with single antigenic peptides. Proc Natl Acad Sci USA 89, 3429–3433.

Hamerman, J.A., and Lanier, L.L. (2006). Inhibition of immune responses by ITAM-bearing receptors. Sci STKE 2006, re1.

Ivashkiv, L.B. (2009). Cross-regulation of signaling by ITAM-associated receptors. Nat Immunol 10, 340–347.

Kerry, S.E., Buslepp, J., Cramer, L.A., Maile, R., Hensley, L.L., Nielsen, A.I., Kavathas, P., Vilen, B.J., Collins, E.J., and Frelinger, J.A. (2003). Interplay between TCR affinity and necessity of coreceptor ligation: high-affinity peptide-MHC/TCR interaction overcomes lack of CD8 engagement. J Immunol 171, 4493–4503.

Laugel, B., Price, D.A., Milicic, A., and Sewell, A.K. (2007). CD8 exerts differential effects on the deployment of cytotoxic T lymphocyte effector functions. Eur J Immunol 37, 905–913.

Lepin, E.J., Bastin, J.M., Allan, D.S., Roncador, G., Braud, V.M., Mason, D.Y., van der Merwe, P.A., McMichael, A.J., Bell, J.I., Powis, S.H., *et al.* (2000). Functional characterization of HLA-F and binding of HLA-F tetramers to ILT2 and ILT4 receptors. Eur J Immunol 30, 3552–3561.

Li, Y., Moysey, R., Molloy, P.E., Vuidepot, A.L., Mahon, T., Baston, E., Dunn, S., Liddy, N., Jacob, J., Jakobsen, B.K., *et al.* (2005). Directed evolution of human T-cell receptors with picomolar affinities by phage display. Nat Biotechnol 23, 349–354.

McCafferty, J., Griffiths, A.D., Winter, G., and Chiswell, D.J. (1990). Phage antibodies: filamentous phage displaying antibody variable domains. Nature 348, 552–554.

McNicol, A.M., Bendle, G., Holler, A., Matjeka, T., Dalton, E., Rettig, L., Zamoyska, R., Uckert, W., Xue, S.A., and Stauss, H.J. (2007). CD8alpha/alpha homodimers fail to function as co-receptor for a CD8-dependent TCR. Eur J Immunol 37, 1634–1641.

Natarajan, K., Dimasi, N., Wang, J., Mariuzza, R.A., and Margulies, D. H. (2002). Structure and function of natural killer cell receptors: multiple molecular solutions to self, nonself discrimination. Annu Rev Immunol 20, 853–885.

Navarro, F., Llano, M., Bellon, T., Colonna, M., Geraghty, D.E., and Lopez-Botet, M. (1999). The ILT2(LIR1) and CD94/NKG2A NK cell receptors respectively recognize HLA-G1 and HLA-E molecules co-expressed on target cells. Eur J Immunol 29, 277–283.

Roberts, M.J., Bentley, M.D., and Harris, J.M. (2002). Chemistry for peptide and protein PEGylation. Adv Drug Deliv Rev 54, 459–476.

Saverino, D., Fabbi, M., Ghiotto, F., Merlo, A., Bruno, S., Zarcone, D., Tenca, C., Tiso, M., Santoro, G., Anastasi, G., *et al.* (2000). The CD85/LIR-1/ILT2 inhibitory receptor is expressed by all human T lymphocytes and down-regulates their functions. J Immunol 165, 3742–3755.

Sewell, A.K., Gerth, U.C., Price, D.A., Purbhoo, M.A., Boulter, J.M., Gao, G.F., Bell, J.I., Phillips, R.E., and Jakobsen, B.K. (1999). Antagonism of cytotoxic T-lymphocyte activation by soluble CD8. Nat Med 5, 399–404.

Veronese, F.M., and Mero, A. (2008). The impact of PEGylation on biological therapies. BioDrugs 22, 315–329.

Willcox, B.E., Gao, G.F., Wyer, J.R., O'Callaghan, C.A., Boulter, J.M., Jones, E.Y., van der Merwe, P.A., Bell, J.I., and Jakobsen, B.K. (1999). Production of soluble alphabeta T-cell receptor heterodimers suitable for biophysical analysis of ligand binding. Protein Sci 8, 2418–2423.

Willcox, B.E., Thomas, L.M., and Bjorkman, P.J. (2003). Crystal structure of HLA-A2 bound to LIR-1, a host and viral major histocompatibility complex receptor. Nat Immunol 4, 913–919.

Willcox, B.E., Thomas, L.M., Chapman, T.L., Heikema, A.P., West, A. P. Jr, and Bjorkman, P.J. (2002). Crystal structure of LIR-2 (ILT4) at 1.8 A: differences from LIR-1 (ILT2) in regions implicated in the binding of the Human Cytomegalovirus class I MHC homolog UL18. BMC Struct Biol 2, 6.

Wyer, J.R., Willcox, B.E., Gao, G.F., Gerth, U.C., Davis, S.J., Bell, J.I., van der Merwe, P.A., and Jakobsen, B.K. (1999). T cell receptor and coreceptor CD8 alphaalpha bind peptide-MHC independently and with distinct kinetics. Immunity 10, 219–225.

Zhang, Y., Liu, Y., Moxley, K.M., Golden-Mason, L., Hughes, M.G., Liu, T., Heemskerk, M.H., Rosen, H.R., Nishimura, M.I., and Gale, M. (2010). Transduction of human T cells with a novel T-cell receptor confers anti-HCV reactivity. PLoS Pathog 6, e1001018.

